

Continuously controlled optical band gap in oxide semiconductor thin films

Andreas Herklotz,^{*,†} Stefania Florina Rus,^{*,‡} and Thomas Zac Ward[†]

[†]ORNL, Materials Science and Technology Division, Bethel Valley Road, Oak Ridge, TN
37831-6056, USA

[‡]Renewable Energies Laboratory - Photovoltaics, National Institute for Research and
Development in Electrochemistry and Condensed Matter, Timisoara 300569, Romania

E-mail: herklotza@gmail.com; rusflorinastefania@gmail.com

Structural characterization

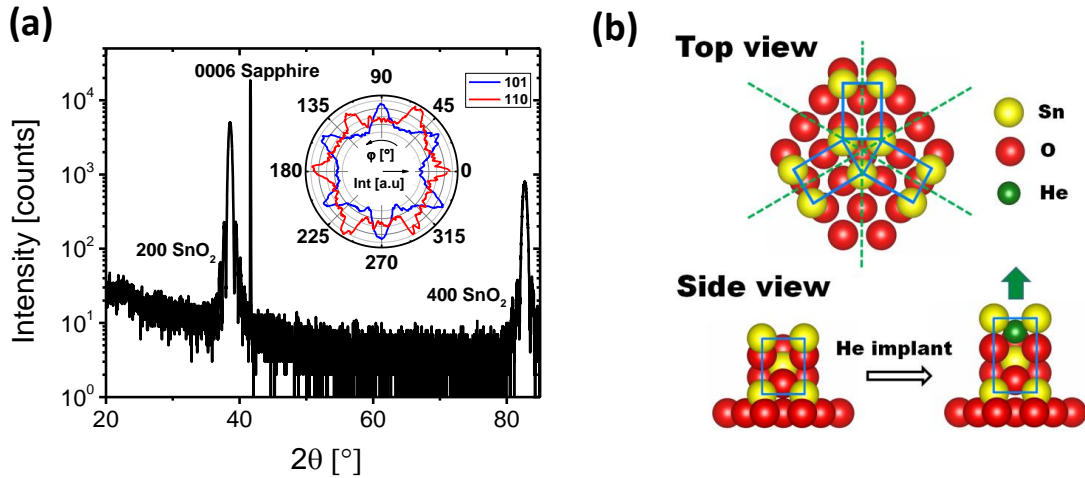


Figure S1: Epitaxial relationship of SnO_2 films: (a) Wide-angle out-of-plane θ - 2θ XRD scan of the undosed SnO_2 film that demonstrates phase-pure epitaxial growth. The inset shows the ϕ -scan on the in-plane 110 (red) and 101 (blue) reflection that reveals 6-fold symmetry. (b) Scheme picturing the in-plane and out-of-plane epitaxy of the films as determined by the XRD experiments.

Fig. S1 (a) shows the X-ray diffraction (XRD) θ - 2θ wide-angle Bragg scan of an undosed

film. The film shows only out-of-plane reflections that can be assigned to the $l00$ peaks of the tetragonal unit cell of SnO_2 . The in-plane epitaxy was determined by ϕ scans around the 110 ($\chi = 45^\circ$) and 101 ($\chi = 56^\circ$) peaks that are characterized by a 6-fold symmetry with a 30° shift between the two lattice reflections (inset). This is expected for growth with a SnO_2 $[010] \parallel \text{Al}_2\text{O}_3 \langle 11\bar{2}0 \rangle$ epitaxial relationship. It means that SnO_2 forms crystallographic domains of about equal portion with the bc plane of the unit cell rotated 120° with respect to each other, as illustrated in the Fig. S1 (b).

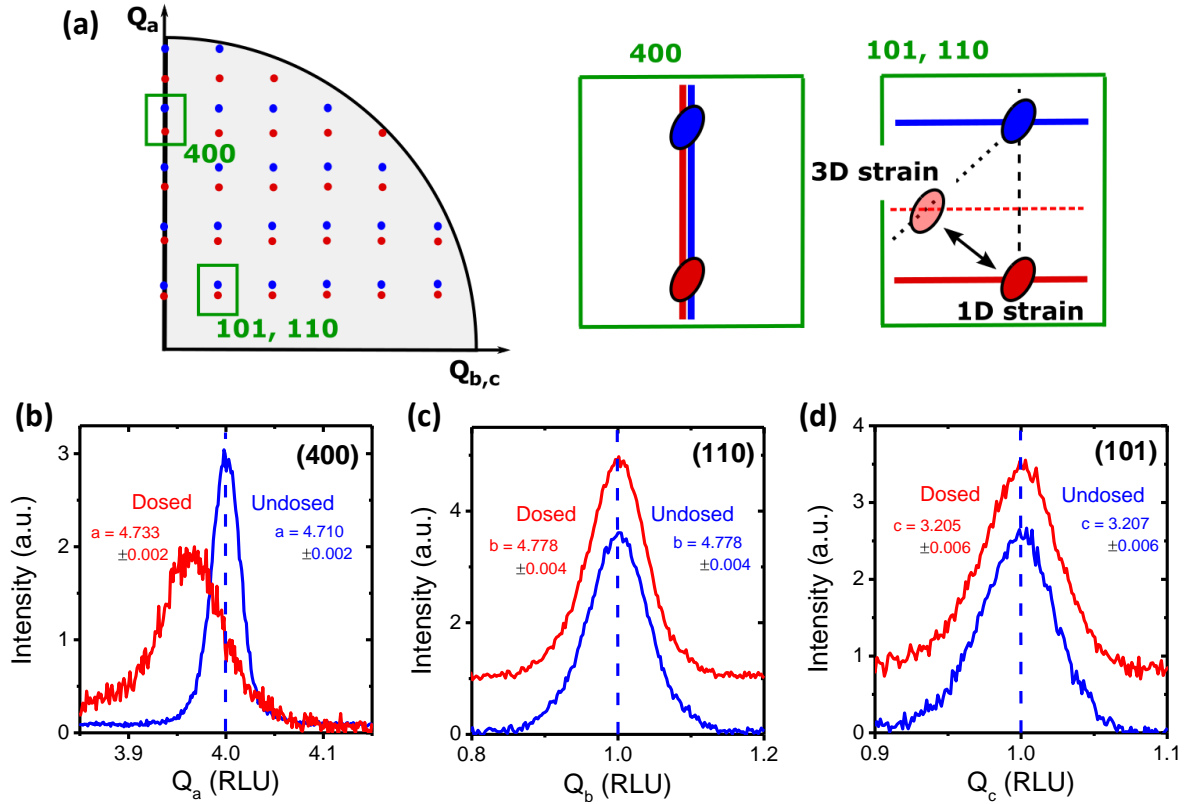


Figure S2: Characterization of lattice expansion: (a) Scheme illustrating the line scans performed on the undosed (blue) and 10×10^{15} He ions/ cm^2 dosed (red) films to determine the oop and ip lattice parameters. In the case of uniaxial oop expansion the in-plane components of the scattering vector remain constant, while in the case of 3D expansion the peak is expected to shift. (b-d) Line scans in reciprocal space through the 400, 110 and 101 reflections of the SnO_2 films, respectively. The components of the scattering vectors are given in reciprocal lattice unit with respect to the undosed film. The oop peak positions are changing upon He implantation, but the ip peak positions remain constant. This confirms that the lattice expansion is uniaxial.

In order to show that the lattice expansion of the SnO_2 upon He implantation is uniaxial

along the oop direction we have performed XRD line scans in reciprocal space. Fig. S2 (b) shows scans for the undosed and 10×10^{15} He ions/cm² dosed film with the scattering vector along the oop direction (Q_a) covering the 400 reflection of the unit cell (see the scheme in Fig. S2 (a) for illustration). The difference in the peak position demonstrates the oop expansion of the unit cell under He doping. Scans in reciprocal space along the in-plane directions (Q_b and Q_c) covering the 110 and 101 reflection are shown in Fig. S2 (c) and (d), respectively. In both cases no peak position change is observed, meaning that the in-plane parameters of the SnO₂ film b and c are not changing upon He implantation. Thus, He doping introduces a single axis oop (1D) strain instead of an expansion in multiple lattice directions. A cubic (3D) expansion would lead to shifts of the peaks to lower Q_b and Q_c values, as illustrated in Fig. S2 (a).

Film morphology before and after He implantation

Fig. S3 (a) shows the AFM image of an as-grown SnO₂ film before the deposition of the Au cap layer. The surface is atomically flat with a root-mean-squared roughness of about 0.1 nm. The AFM images in Fig. S3 (b) depict the surface of the undosed film where the Au cap layer was deposited and removed subsequently without He implantation, whereas Fig. S3 (c) shows the surface of the film that was dosed with 10×10^{15} He ions/cm². Both films have surfaces of equal quality. This proves that ion sputtering effects are limited to the first few nm of the Au cap layer and the atomically sharp SnO₂ surface is revealed after the mechanical removal of the cap layer. Note that this mechanical removal of the sputtered Au layer leaves scratches on the film surface as seen in both AFM images. However, the scratches have a negligible influence on the optical properties of the films and this method was preferred to a chemical wet etch that could seriously affect the chemical and topographic state of the film surface. We note that presented data for optical properties were all taken on films that had an Au cap and mechanical removal regardless of whether they were dosed or undosed. As-grown films were also characterized without Au cap and found to behave identically to undosed films after Au cap removal.

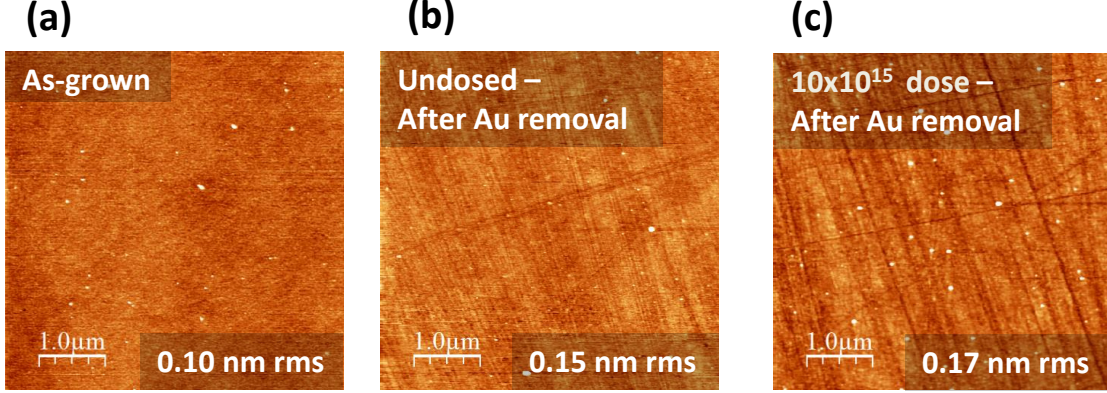


Figure S3: AFM images of the SnO_2 surfaces (a) before the deposition of the Au cap layer, (b) after removal of the Au cap layer without He implantation and (c) after removal of the Au cap layer after the film was implanted with 10×10^{15} He ions/ cm^2 . The height scale is the same for all images.

Ellipsometry models

The ellipsometric parameters ψ and δ determined by VASE were fitted by a simple two layer model consisting of the SnO_2 film and the sapphire substrate. The optical constants of the sapphire substrates have been determined in a separate measurement and have been fixed. The SnO_2 layer was fitted by a Kramers-Kronig consistent B-spline model with a node spacing of 0.2 eV. Figure S4 (a) shows the fits (blue) to the experimental data (orange and gray) for the undosed film. The mean square error (MSE) is low, which means that the fit result is in good agreement with the data. Figure S4 (b) shows the fit for the film dosed with 10×10^{15} He ions/ cm^2 and also illustrates the good match with the data. In order to demonstrate the significance of the changes induced by He implantation, the experimental data of the undosed film is shown for comparison (dashed red lines). The data of the dosed film can be fitted satisfactorily by a simple two layer model. This demonstrates that the optical properties of the dosed SnO_2 film can be approximated by an homogeneous layer. In order to corroborate this fact, a three layer model was applied (c) that introduces a second SnO_2 layer and could account for a lower He dosed part of the film near the interface or the surface or incorporate sputter effects. This three layer model results in a fit that is improved only insignificantly. We therefore conclude that the He dosed film-substrate system can be

adequately approximated by a two layer model without any surface or interface roughness.

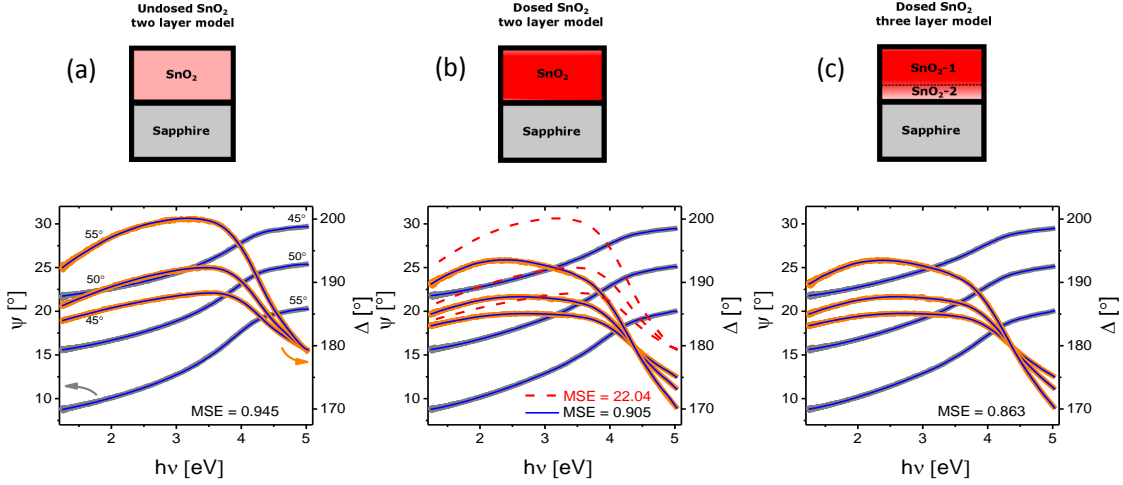


Figure S4: Ellipsometric parameters ψ and Δ in dependence of the incident angle of the reflected light and the photon energy for the undosed film (a) and the film dosed with 10×10^{15} He ions/cm² (b and c). Fitting the experimental data (orange and grey) with a two layer model (a and b) consisting of the SnO_2 film and the sapphire substrate provides good results. In (c) the data of the dosed film is fitted by a three layer model. The mean squared error (MSE) is only slightly smaller than that of the two layer model. In (b) the experimental ψ data of the undosed film is shown in order to illustrate the changes induced by He implantation.

Optical properties

Fig. S5 (a) shows the dependence of the refractive index n on the wavelength over the full measured spectral range. The refractive index is consistently decreasing with increasing He dose. In general, the refractive index is influenced by the density and the local polarizability.¹ The strain-induced increase of the unit cell is reducing the optical density of the SnO_2 film and thereby decreasing the refraction. Moreover, due to the vanishing electronegativity, helium can only contribute to changes in the polarizability, but the increased Sn-O bond lengths will lead to an overall reduction of the polarizability that is reflected in a decreased refractive index.² An approximately linear shift of the maximum of n near 290nm to higher wavelength is found upon He implantation. This peak is related to the optical inter-bandgap transition of SnO_2 .³ The redshift further corroborates the strain-induced decrease of the band gap. The extinction coefficient k , as shown in Fig. S5 (b), is generally increasing with

He dosing. It should be noted that this increase is not related to the creation of defects, which would introduce narrow absorption bands below the band gap or even a plasmon band in the infrared region, which we do not observe. The dosing effect over the full wavelength rather indicates that the increased k is a result of light scattering at He sites.⁴

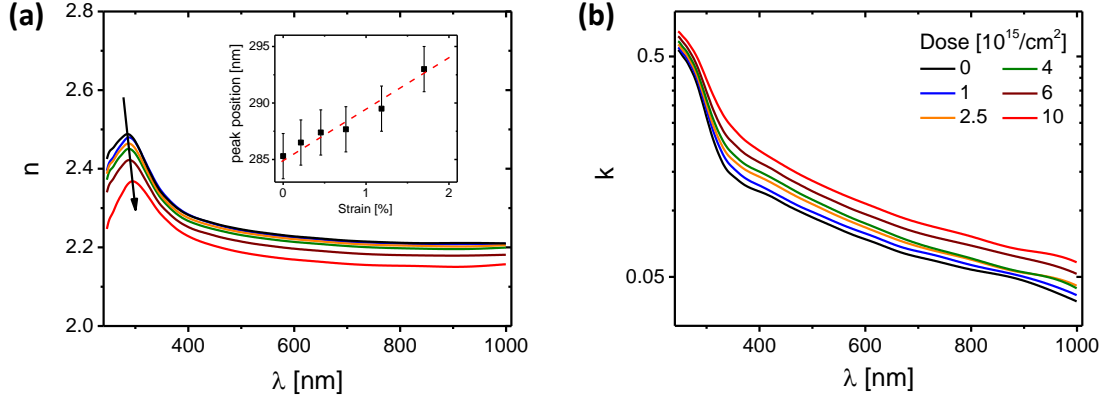


Figure S5: Optical constants of He implanted SnO_2 films: (a) refractive index and (b) extinction coefficient as function of the wavelength λ for various He doses. The arrow indicates the redshift of the refractive index peak as shown in the inset.

References

- (1) Townsend, P. D. *Reports on Progress on Physics* **1987**, *50*, 501.
- (2) Pan, S. S.; Zhang, Y. X.; Teng, X. M.; Li, G. H.; Li, L. *Journal of Applied Physics* **2008**, *103*, 093103.
- (3) Kei, C.; Yang, Z.; Zhu, W.; Pan, J. S.; Karamat, S. *Journal of Applied Physics* **2010**, *107*, 013515.
- (4) Cummings, H.; Levanyuk, A. *Light Scattering Near Phase Transitions*; Elsevier Science Publishing Company: New York, 1983.